J Fluoresc (2015) 25:685–694
DOI 10.1007/s10895-015-1554-9

ORIGINAL PAPER

DFT Studies of the Photophysical Properties of Fluorescent and Semiconductor Polycyclic Benzimidazole Derivatives

Umesh Warde · Lydia Rhyman · Ponnadurai Ramasami · Nagaiyan Sekar

Received: 12 December 2014 / Accepted: 5 March 2015 / Published online: 26 March 2015
© Springer Science+Business Media New York 2015

Abstract The photophysical and electrochemical properties of eleven polycyclic benzimidazole fused organic pigments (four based on phthalic anhydride, four based on naphthalic anhydride and three based naphthalene tetra carboxylic acid dianhydride) were investigated using density functional theory and time dependent density functional theory methods (B3LYP/6-31G(d) and M06/6-31G(d)). The predicted geometries are comparable using both functionals. The electrochemical properties are in good agreement with the experimental results. However, the experimental absorption-emission properties are closer to the values computed using the M06/6-31G(d) method. Both the methods perform equally well in explaining the intramolecular charge transfer characteristics. This work can help to understand the modern age functional materials at molecular level and to design new molecules.

Keywords Polycyclic benzimidazole · DFT · TD-DFT · HOMO-LUMO · Organic semiconductors · Hyperpolarizability

Electronic supplementary material The online version of this article (doi:10.1007/s10895-015-1554-9) contains supplementary material, which is available to authorized users.

U. Warde · N. Sekar (✉)
Tinctorial Chemistry Group, Department of Dyestuff Technology, Institute of Chemical Technology, N. P. Marg, Matunga, Mumbai, MH, India 400019
e-mail: n.sekar@ictmumbai.edu.in

N. Sekar
e-mail: nethi.sekar@gmail.com

L. Rhyman · P. Ramasami (✉)
Computational Chemistry Group, Department of Chemistry, Faculty of Science, University of Mauritius, Réduit 80837, Mauritius
e-mail: ramchemi@intnet.mu

P. Ramasami
Department of Pharmaceutical Chemistry, College of Pharmacy, King Saud University, P.O. Box 2457, Riyadh 11451, Saudi Arabia

Introduction

Naphthalene tetra carboxylic acid and perylene tetra carboxylic acid monobenzimidazoles and their bis analogues (NTCBI and PTCBI) are important from an industrial point of view as organic pigments [1, 2] and n-type organic semiconductors [3]. These compounds have been extensively studied and applied in organic electronics owing to their stability, efficient light absorbance and good electron transportation characteristics. Naphthalene diimide derivatives of these compounds have already shown their promising optoelectronic properties [4–6]. These compounds can be useful in devices such as light-emitting diodes [7], organic thin-film transistors (OTFTs) [8, 9], organic photovoltaic's (OPVs) [10, 11], organic electronics [12] and organic field effect transistors (OFET) [13–15].

These kind of functional materials have some basic molecular properties such as good reduction/oxidation potentials and solid-state crystal packing to enhance electron transportation properties. The design and synthesis of such compounds are important area of research. Computational approach using density functional theory (DFT) method and its time dependent version (TD-DFT) have been an effective tool to understand the molecular basis of photophysical as well as other electronic properties driven by the interaction of electromagnetic impulses with organic compounds [16]. In 2011, Anzenbacher Jr. et al. [17] reported an elegant green synthesis of polycyclic benzimidazole derivatives as potential organic semiconductors. They also investigated the photophysical and

electrochemical properties of these materials. However, there are no studies involving the interpretation of the geometrical, photophysical, electrochemical and semiconductor properties of these compounds at molecular level. Therefore, to complement the literature of the polycyclic benzimidazole derivatives, in this paper, we report for the first time, quantum mechanical computations of eleven polycyclic benzimidazole fused organic pigments, Fig. 1. (four based on phthalic anhydride, four based on naphthalic anhydride and three based on naphthalene tetracarboxylic acid dianhydride). The present paper highlights the comparison between experimentally observed photophysical and electrochemical results [17] with the data computed using DFT and TD-DFT methods. We also discuss the effect of geometrical parameters affecting the charge transfer properties of these compounds.

Computational Methods

All the computations were performed using the Gaussian 09 package [18] running on GridChem [19]. Ground state (S0) geometry of the compounds was optimized without imposing symmetry in the gas phase using DFT method [20]. The functionals used were the old but the popular B3LYP and new the generation M06. The B3LYP functional combines Becke's three Parameter exchange functional (B3) [21–24] with the non-local correlation functional by Lee, Yang and Parr (LYP) [25–27]. The M06 functional is one of the sets of four meta-hybrid GGA DFT (Generalized gradient approximation) functionals which is highly parameterized accounting for non-covalent interactions as well as "medium range" electron correlations. The M06 functional has 27 % Hartree-Fock exchange and it is known to perform well when non-covalent interactions are present as against the B3LYP functional [28, 29]. The basis set used for all atoms was 6-31G-(d). The Polarizable Continuum Model (PCM) [30, 31] was used to optimize the ground and excited state geometries in dichloromethane (DCM). The vibrational frequencies were computed for the optimized geometries to investigate the nature of the stationary points. The optimized structures were confirmed to be the local minima on the potential energy surface and no imaginary frequencies were noted. The vertical excitation energies and oscillator strengths were obtained for the lowest 20 singlet-singlet transitions at the optimized ground state equilibrium geometries by using the TD-B3LYP/6-31G(d) and TD-M06/6-31G(d) methods [32–34].

The low-lying first singlet excited states (S1) of all the benzimidazole compounds were relaxed to obtain their minimum energy geometry. The vertical emissions were computed using TD-DFT method with the optimized first singlet excited state geometry [35, 36]. Frequency computations were also carried out on the low lying first singlet excited state of the compounds. The vertical electronic excitation spectra, including wavelengths of absorption, oscillators strengths, and main configuration assignment, were systematically investigated using the TD-B3LYP/6-31G(d) and TD-M06/6-31G(d) methods.

Results and Discussion

Geometrical Parameters

The charge transfer characteristics are influenced by the geometry of the compounds. The optimized geometries of the eleven molecules can be interpreted with the help of the basic

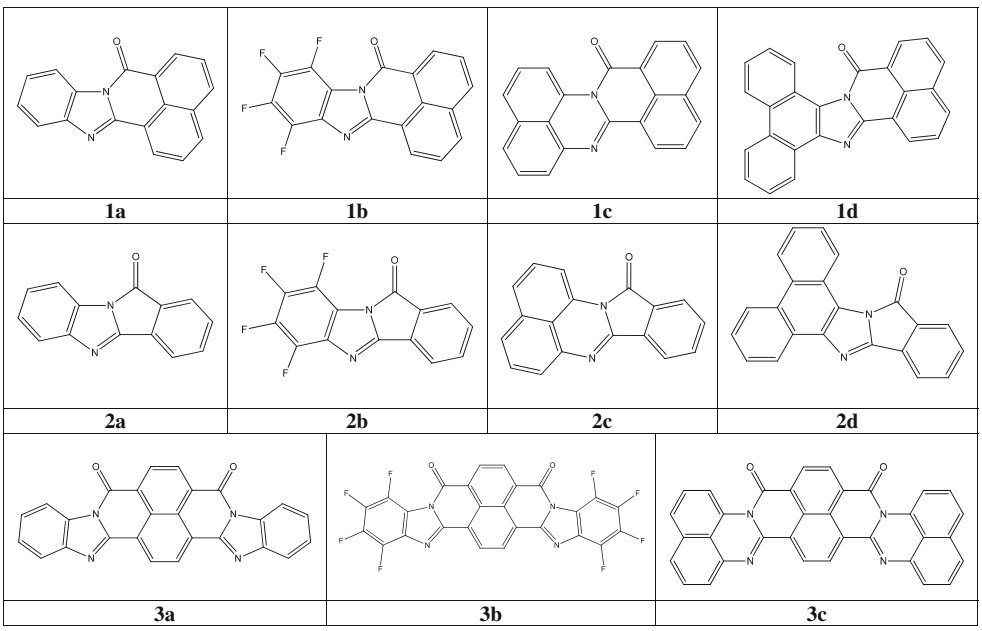

Fig. 1 Structures of the compounds studied

structure as shown in Fig. 2. The dihedral angle, bond angle and bonds which show prominent changes in the first singlet excited state compared to the ground state are also illustrated (Fig. 2). The two nitrogen atoms forming the imidazole or pyrimidine unit (designated as C-core) are anchored on one side with the carbonyl containing aryl core originating from the anhydrides (designated as A-core in Fig. 2) and on the other side another aryl core originating from the 1,2-diamine (designated as D-core). The dihedral angles which the C-core bears on both sides (in the ground and in the excited states) are influenced by the substituents on both cores as well as the nature of the anhydride.

Both the hybrid functionals predicted that the compounds **1a, 1b, 2a-2d, 3a** and **3b** have planar geometry, while the compounds **1c, 1d** and **3c** have twisted geometry in both the ground and excited states. In the case of compounds **1a** and **1b**, the C1-N1-C3-C4 dihedral angle is close to zero and the angles C1-N1-C3-C6 and C1-N1-C2-N2 (Fig. 2) are close to 180° respectively in both the ground state and the first singlet excited state. The bond angle around the carbonyl carbon (N1-C1-C5) for compound **1a** is found to be 114° in the ground state and 113° in the excited state. These deviations from the expected 120° can be explained in terms of the strain associated with the five membered imidazole moiety. The difference is only 0.7° suggesting that there is no significant change in the planarity on excitation to the first singlet excited state as predicted by the M06 functional while B3LYP functional predicts a difference of 0.8°. Similar results regarding the dihedral angles (supporting information) are observed in the case of the compound **1b** suggesting that there is no significant difference due to the presence of more electronegative fluorine atom (compared to the hydrogen) on the planarity of the molecule.

In the case of the compound **1c** (twisted geometry), C1-N1-C3-C4 dihedral angle is found to be deviated in the excited state. The M06 functional computed this deviation to be larger as compared to the B3LYP functional. The results are similar for C1-N1-C2-N2 and C1-N1-C3-C6 dihedral angles (should be 180°) as C1-N1-C3-C4. The N1-C1-C5 bond angle is found to decrease in the excited state compared to the ground state by 1.5° in the B3LYP-optimized geometry and by 1.3° in the M06-optimized geometry. The N1-C1-C5 bond angle for compound **1d** is found to be deviated in the excited state compared to the ground state by 0.6° as computed by both functionals. Similar results are found for the C1-N1-C2-N2 and C1-N1-C3-C6 dihedral angles for the compounds **1c** and **1d**. These observations suggest that the compounds **1c** and **1d** which are twisted both in the ground and excited state but attain some planarity in the excited state compared to the ground state.

For the series of compounds **2a-2d**, the C1-N1-C3-C4 dihedral angle is observed to be close to zero and C1-N1-C3-C6 and C1-N1-C2-N2 dihedral angles are observed to be close to 180° in the ground and excited states, respectively. The N1-C1-C5 bond angle is found to decrease in the excited state compared to the ground state by 2–2.5° using the M06 functional. These trends are not different for B3LYP functional (Supporting information).

In the case of the bis-benzimidazole derivatives **3a** and **3b**, both the functionals predict that the N1-C1-C5 bond angle is similar to the other planar compounds (**1a, 1b, 2a-2d**). The C1-N1-C3-C4 dihedral angle is observed close to zero and C1-N1-C3-C6 and C1-N1-C2-N2 angles are observed to be close to 180° in both the ground and in the excited states. The N1-C1-C5 bond angle in compound **3c** (twisted geometry) is found to be 117.3° in the ground state and 116.6° in the excited state as predicted by the B3LYP functional. The same angle is observed to be 116.7° in the ground state and 116.5° in the excited state as predicted by the M06 functional. This is close to the expected value of 120° which is not observed for the mono-imidazoles **1c** and **1d**. The difference in the C1-N1-C3-C4 dihedral angle between the ground and excited states are 0.6° and 2.3° using the B3LYP and M06 functionals, respectively. The other C1-N1-C3-C6 and C1-N1-C2-N2 dihedral angles are found to increase in the excited state as compared to ground state. However, the difference is larger in the M06-optimized geometry as compared to the B3LYP-optimized geometry (Table 1). This shows that the M06 functional predicts planar structure in the excited state unlike the structure optimized using the B3LYP functional.

Additional information regarding the bond lengths of the eleven compounds is summarized in the Tables 1.1-3.3

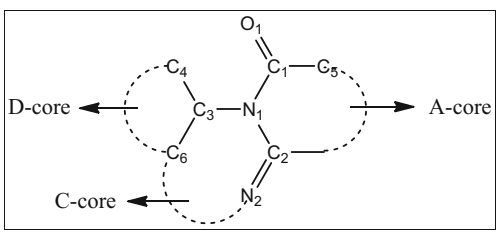

Fig. 2 General structure of the eleven compounds studied

Table 1 Twisted dihedral angle predicted using the hybrid functionals (B3LYP and M06) of compounds **1c**, **1d** and **3c** in the ground state (GS) and excited state (ES) optimized geometry in DCM

Dihedral angle in °	Functional	1c		1d		3c	
		GS	ES	GS	ES	GS	ES
C1-N1-C3-C4	B3LYP	20.0	18.0	18.41	15.8	18.0	17.4
	M06	21.3	18.0	23.1	19.0	21.2	18.9
C1-N1-C3-C6	B3LYP	161.5	165.1	166.9	170.0	163.4	164.8
	M06	160.4	165.3	163.4	167.8	160.6	163.7
C1-N1-C2-N2	B3LYP	162.7	165.6	168.5	171.4	164.4	165.9
	M06	161.8	166.1	165.2	169.4	161.7	164.6

(Supporting Information). In the case of the **1a-1d**, **2a-2d** and **3a-3c**, the major bond lengthening is observed for the C1-N1, C2-N2, N1-C2 and C3-C6 bonds (Fig. 2). The major lengthening of the C1-N1 bond observed in the compound **1c** is found to be 0.054 Å (M06 functional) and 0.065 Å (B3LYP functional) in the excited state. This means that due to charge transfer in the excited state the C1-N1 bond lengthening is significant for the compounds **1a, 1b** and **1d**. Similar observation and explanation apply for the observed increase in the C1-N1-C2-N2 dihedral angle in the excited state compared to the ground state and thus attaining planarity due to charge transfer. Bond lengths are increased in the excited state as compared to the ground state by about 0.018-0.040 Å for the C2-N2, N1-C2 and C3-C6 bonds for the compounds **1a-1d** while the C1-C5 and N1-C3 bonds are shortened (Fig. 2).

The trend in the bond lengthening observed for the C1-N1 bond in the compounds **2a-2d** is similar as for compounds **1a-1d**. The C1-N1 bond is also found to be increased by 0.074 and 0.080 Å in the excited state as compared to the ground state predicted by both the M06 and B3LYP functionals, respectively. The other C2-N2, N1-C2 and C3-C6 bonds are found to be increased by 0.027-0.040 Å in the case of the compounds **2a**, **2b** and **2d**. The C1-C5 and N1-C3 bonds are shortened for the compounds **2a-2d**. Analogous results are also observed in the case of the compounds **3a-3d**. The bond lengths predicted by the B3LYP functional are longer as compared to the M06 functional. It is clear from the above observation regarding the bond lengths that the twisted compounds (**1c**, **1d** and **3c**) show major differences in the bond lengths in the excited state as compared to ground state.

Electronic Vertical Excitation Spectra

The computed vertical excitation spectra along with their oscillator strengths, composition of the orbitals associated with the transition for the chromophore as well as the corresponding experimental absorption wavelengths [17] are shown in Table 2. The M06 and B3LYP functionals predict that the compounds **2a** and **2b** show major electronic transition (considering experimental values) HOMO-1 to LUMO, while the remaining compounds show major electronic transition from HOMO to LUMO. The compounds **2a** and **2b** absorption bands occur at lower energy with higher oscillator strength compared to other compounds. This is due to the intramolecular charge transfer (ICT) which is significant for compounds **2a** and **2b.** These ICT bands are mainly due to the electronic transition from the HOMO-1 and HOMO to the LUMO respectively. The compounds **2a**, **2b** and **1b** have the absorption values 330, 337 and 389 nm predicted by the M06 functional which are in good agreement with the experimental values 340, 337 and 382 nm respectively. Absorption values predicted by the M06 functional for the compounds **3a-3c** are in fair agreement with the experimental values with good oscillator strength. The absorption values predicted by the B3LYP functional show larger deviations as compared to the values predicted from the M06 functional (Table 2). The oscillator strengths predicted by the M06 functional are higher as compared to the B3LYP functional (Table 2).

The experimentally found UV–vis spectra of compounds **1a-1d** and **3a-3c** are characterized by broad π-π* transition with an extinction coefficient in the range of 8000 M^{-1} cm^{-1} [17]. The broad π-π* transition in the compounds of the series **3** has been explained in terms of aggregation in dichloromethane [17]. The optimized geometry in dichloromethane using the PCM model gives a similar broad vertical excitation. The π-π* transition bands of **1a** and **1b** have been located at 350–420 nm experimentally. Similar π-π* transitions for the compounds **1c** and **1d** have been located at 390–600 and 370–500 nm respectively. All these observations are supported by the TD-DFT computed vertical excitations with the B3LYP and M06 functionals.

Emission Spectra

The computed emission for the eleven compounds along with experimental values [17] are given in Table 3. In the case of the compounds **1a-1d** and **3a** and **3b**, the emission energy correlates with the quantum efficiency (energy gap law) [37, 38]. This effect is apparent for the compounds **1a**,**1b** and **3a**, **3b** which differ only in the C-H and C-F bonds [17]. The electron withdrawing fluorine atom induces a 33 nm blue shift in the **1b** emission maximum as compared to **1a**. The effect of the electronegativity of fluorine atoms on the emission of **3b** results in a 36 nm blue shift as compared to **3a** [17]. The M06 functional predicted this blue shift as 20 nm for **1b** as compared to **1a** and as 49 nm in case of the **3b** as compared to **3a**, which is in fair agreement with the experimental values. The B3LYP functional on the other hand has predicted this blue shift as 10 nm for **1b** as compared to **1a** which is low and as 98 nm blue shift for **3b** as compared to **3a** which is higher compared to experimental value.

The computed fluorescence emission results obtained using the TD-M06/6-31G(d) method are fairly in good agreement with the experimental emission maximum because the deviation is generally less than 10 %. The M06 functional has lower values emission values but they are close to experimental results for the compounds **1a-1d**, whereas for the B3LYP functional these values are found to be higher as compared to the experimental values. For the compounds **2a-2d** the emission energies are found to be lower using the M06 functional. The B3LYP functional also predicts the same trend of higher emission values (Table 3) except for the compound **2d** which is found to be higher compared to the experimental values. Both the functionals predict slightly larger emission energy values for compounds **3a** and **3b** (bis-benzimidazole derivative) as compared to the experimental values. The

Table 2 Observed UV-Visible absorption and vertical excitation properties for all the eleven compounds in dichloromethane computed using M06 functional

Sr. No.	Compound	λ_{max}[a] nm	Computed vertical excitation properties							
			TD-B3LYP				TD-M06			
			Vertical excitation[b]	f[c]	Orbital contribution	%D[d]	Vertical excitation[b]	f[c]	Orbital contribution	%D[d]
1	**1a**	384	429.5	0.26	H→L (96 %)	11	413.9	0.32	H→L (97 %)	8
2	**1b**	382	404.9	0.37	H→L (97 %)	6	389.1	0.43	H→L (98 %)	2
3	**1c**	475	522	0.33	H→L (98 %)	9	511.6	0.05	H→L (98 %)	8
4	**1d**	436	493.9	0.2	H→L (98 %)	0.13	469.1	0.22	H→L (98 %)	7
5	**2a**	340	342.5	0.2	H-1→L (96 %)	0.7	330.5	0.18	H-1→L (88 %)	3
6	**2b**	337	356.6	0.2	H-1→L (72 %)	6	337.9	0.21	H-1→L (78 %)	0.3
7	**2c**	448	484	0.3	H→L (96 %)	8	469.2	0.28	H→L (96 %)	5
8	**2d**	441	503.7	0.1	H→L (98 %)	14	484.8	0.08	H→L (98 %)	10
9	**3a**	484	442.4	0.08	H→L (97 %)	8	539.9	0.59	H→L (98 %)	11
10	**3b**	471	456.2	0.02	H-1→L (98 %)	3	513.3	0.70	H→L (98 %)	9
11	**3c**	609	625.3	0.04	H-1→L (98 %)	3	665.0	0.80	H→L (99 %)	9

[a] Experimental absorption wavelength in nm

[b] Computed absorption wavelength in nm

[c] Oscillator strength

[d] % Deviation between experimental absorption and computed vertical excitation

emission energy is predicted to be close to experimental values for the twisted compounds **1c** and **1d** by the M06 functional compared to B3LYP functional. The emission energy obtained from the M06 functional is closer to the experimental results [17] compared to those obtained from the B3LYP functional.

Computed HOMO-LUMO Energy Values and Electrochemical Properties

The computed energies of HOMO and LUMO of the compounds and the experimental cyclic voltammetry data are summarized in Table 4. It is observed that the B3LYP functional predicts HOMO energy values closer to the experimental findings, while the M06 functional underestimates the HOMO energy values. On considering the LUMO energy, it was found that the values are larger in magnitude (M06 functional) as compared to the experimental values and even more than the values computed with the B3LYP functional.

It was reported [17] that the fluoro derivatives **1b**, **2b** and **3b** have higher electron affinity compared to the other derivatives in the series of compounds **1**, **2** and **3**. Similar results (HOMO and LUMO values in Table 4) are predicted from both the B3LYP and M06 functionals. Experimentally, it was observed that even though naphthalene and phenanthrene derivatives **1c** and **1d** exhibit similar LUMO energy, the red shift in absorption in **1c** is due to the low-lying HOMO level [17]. Results from both the functionals are comparable and follow similar trend (Table 4). The HOMO level of **1a** is similar to **3a** and that of **1b** is similar to **3b** [17]. Experimentally (Table 4) the compounds **3a**-**3c** show the LUMO levels are deeper (ca. 0.7–0.8 eV - calculated difference in LUMO

Table 3 Observed UV-Visible emission and vertical excitation properties for the eleven compounds in dichloromethane computed using M06 functional

Sr. No.	Compound	Experimental λ_{max}[a] nm emission	Computed emission			
			TD-B3LYP		TD-M06	
			Emission λ_{max}[b] nm	% D[c]	Emission λ_{max}[b] nm	% D[c]
1	**1a**	499	519	4	492	1.4
2	**1b**	466	509	9	472	1.3
3	**1c**	682	691	2	643	5.7
4	**1d**	589	624	7	582	1.1
5	**2a**	519	557	8	536	3.2
6	**2b**	485	537	10	514	6.0
7	**2c**	596	636	8	613	3.0
8	**2d**	616	503	23	647	5.0
9	**3a**	585	749	32	701	20.0
10	**3b**	549	647	19	652	19.0
11	**3c**	NE	761			

NE Not estimated

[a] Experimental emission wavelength in nm

[b] Computed emission wavelength in nm

[c] % Deviation between experimental absorption and computed emission

Table 4 Experimental cyclic voltammetry results and computed HOMO-LUMO values of the compounds in dichloromethane in electron volt (eV)

Compound	Experimental		M06 functional		B3LYP functional	
	HOMO (eV)	LUMO (eV)	HOMO (eV)	LUMO (eV)	HOMO (eV)	LUMO (eV)
1a	−5.86	−3.06	−6.23	−2.39	−5.95	−2.53
1b	−6.06	−3.16	−6.43	−2.54	−6.13	−2.68
1c	−5.07	−2.96	−5.52	−2.32	−5.22	−2.45
1d	−5.51	−3.08	−5.82	−2.42	−5.54	−2.57
2a	−5.84	−2.98	−6.54	−2.28	−6.24	−2.44
2b	−6.18	−3.15	−6.84	−2.52	−6.53	−2.67
2c	−5.21	−2.94	−5.69	−2.28	−5.40	−2.42
2d	−5.39	−3.05	−5.89	−2.38	−5.61	−2.54
3a	−5.79	−3.37	−6.26	−3.27	−5.96	−3.38
3b	−6.01	−3.92	−6.55	−3.48	−6.24	−3.59
3c	−5.17	−3.63	−5.55	−3.08	−5.25	−3.18

values between series **3** and **1**) [17] compared to compounds **1a-d** [17], while the M06 and B3LYP functionals predict this value to be 0.7–0.9 eV. The lower HOMO-LUMO energy gap enhance better electron transportation and thereby indicating that these compounds have good semiconductor properties. The bis-benzimidazole derivatives of compounds **3** are found to have lower HOMO-LUMO gap compared to their mono analogues of compounds **1**. Our theoretical results are in agreement with the experimental HOMO-LUMO gap calculated by cyclic voltammetry reduction potential [17].

Frontier Molecular Orbitals (FMOs)

The effect of the charge transfer from phenyl, naphthalene and phenanthrene ring as donor and carbonyl chromophore as acceptor is studied by examining the HOMO and LUMO surfaces of the eleven compounds. The first dipole-allowed electronic transitions, and the strongest electron transitions with largest oscillator strength, correspond to the promotion of an electron from HOMO→LUMO. To understand the above electronic transitions, the surfaces of the HOMOs and LUMOs were generated by using GaussView 9.0 software [39]. Fig. 3 displays the energies of the different molecular orbitals involved in the electronic transitions of the representative three classes of compounds (**1b**, **2c** and **3a**) in dichloromethane obtained from the B3LYP-optimized and M06-optimized geometries. From Fig. 3, it can be seen that the electron density of the HOMO lies on the two nitrogen atoms and the donor (Core-D) ring in **2c** and **3a** respectively, which shifts onto the carbonyl group and the C-core (Figs. 2 and 3) of the LUMO. This indicates the charge transfer behavior of the compounds whereby the electrons are pulled from the donor to the acceptor. It is also found that there is no charge density in the LUMO of these compounds and that there is a node between the bonding atoms.

In the case of the compounds **1b** and **3a,** the electron density is completely shifted on the acceptor part of the compounds while in the case of **2c** there is still some electron density on the naphthalene ring of the donor. This means that the charge is not efficiently transferred in compound **2c** which is also in agreement with the lower value of oscillator strengths of absorption (0.278) as compared to **1b** (0.439) and **3a** (0.593) as computed by the M06 functional. Oscillator strength predicted from the TD-B3LYP method of **3a** (0.090) is lower than that of **2a** (0.170) and **2c** (0.260). Similar observations are found for other compounds.

Static Second-Order Nonlinear Optical (NLO) Properties

Organic nonlinear optical (NLO) materials are at present attracting considerable interest as an alternative to the inorganic materials. The donor-π-acceptor molecules have been effectively used in the development of the second-order organic NLO materials [40]. Most of the materials reported to date have n-electron conjugated systems, which are the main origin of their optical nonlinearities [41]. The compounds reported in this paper do not have the push-pull chromophores but they have good semiconductor properties. Hence, their NLO properties have been studied using DFT method to complement the literature and to aid experimentalists in the synthesis of these compounds.

Here, the second-order NLO properties of the polycyclic benzimidazole and bis-benzimidazole derivatives were calculated. The static second-order polarizability or first hyperpolarizability (β) and its related properties for compounds **1a**-**1d**, **2a**-**2d** and **3a**-**3c** were calculated on the basis of the finite-field approach [42]. In the presence of an applied field, the energy of the system is a function of the electric field, and the hyperpolarizability is a third rank tensor that can be described by a $3\times3\times3$ matrix which is dependent on the

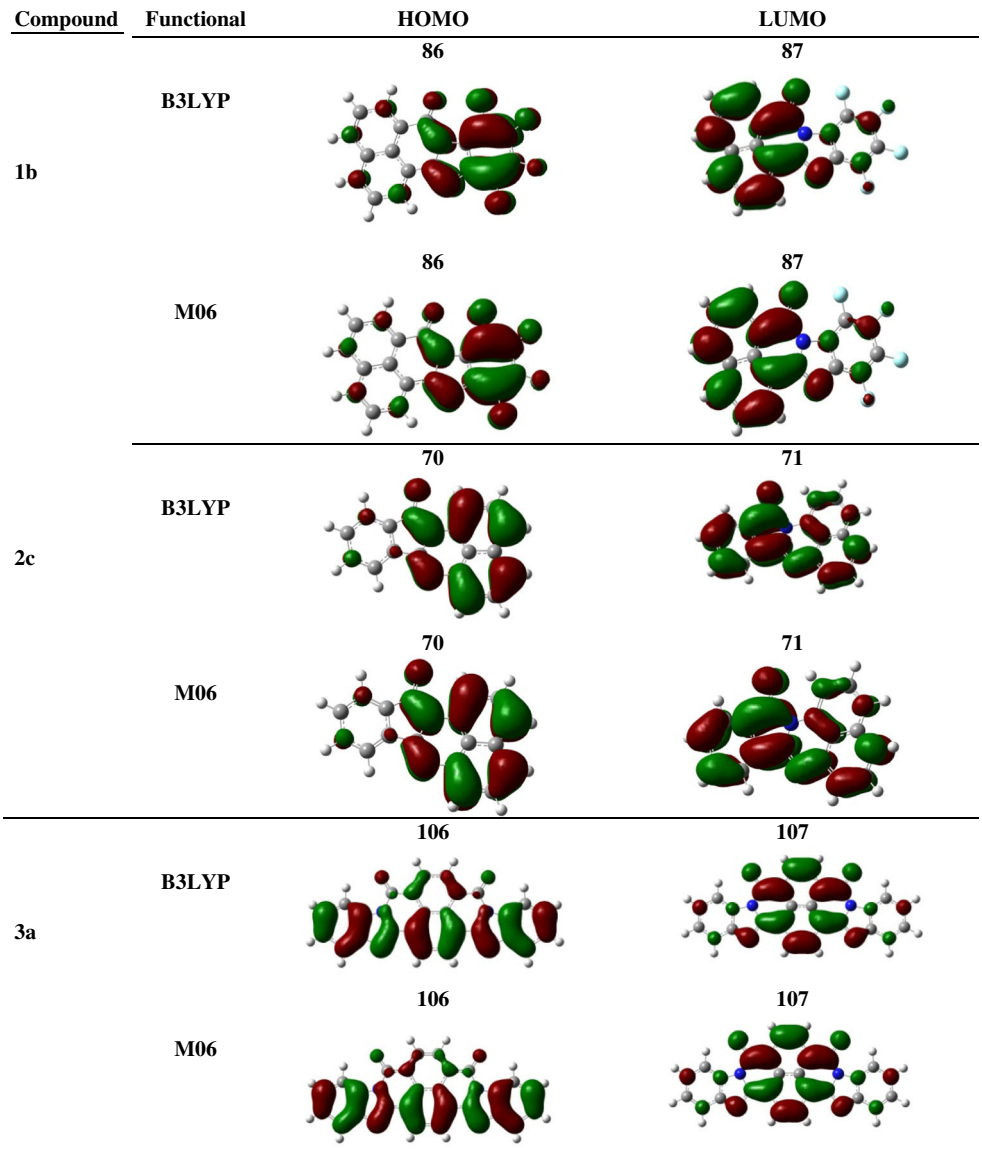

Fig. 3 Frontier molecular orbitals of the compounds **1b**, **2c** and **3a** in the ground and excited states

method used. The 27 components of 3D matrix can be reduced to 10 components due to Kleinman symmetry [43]. The matrix can be given in the lower tetrahedral format. It is obvious that the lower part of the 3×3×3 matrices is a tetrahedral. The components of β are defined as the co-efficient in the Taylor series expansion of the energy in the external electric field. When the external electric field is weak and homogeneous, this expansion becomes:

$$E = E^{\circ} - m_a F_a - 1/2 a_{ab} F_a F_b - 1/6 b_{abg} F_a F_b F_g + \ldots\ldots\ldots (1)$$

where E° is the energy of the unperturbed molecules, Fα is the field at the origin, μα, ααβ and βαβγ are the components of dipole moment, polarizability and the first hyperpolarizabilities, respectively. The complete equations for calculating the magnitude of total static dipole moment (μ), the mean polarizability (α_0), the anisotropy of the polarizability ($\Delta\alpha$) the mean first hyperpolarizability (β) and static second hyperpolarizability (γ), using the *x*, *y*, *z* components from Gaussian 09 W output are defined as follows [44]:

$$\mu = \left(\mu_x^2 + m_y^2 + m_z^2\right)^{1/2} \quad (2)$$

$$a_0 = (1/3)a_{xx} + a_{yy} + a_{zz} \quad (3)$$

$$\Delta\alpha = 2^{-1/2}\left[\left(\alpha_{xx} - \alpha_{yy}\right)^2 + \left(\alpha_{yy} - \alpha_{zz}\right)^2 + \left(\alpha_{zz} - \alpha_{xx}\right)^2 + 6\alpha_{xx}^2\right]^{1/2} \quad (4)$$

$$\beta_{total} = \left[\left(\beta_{xxx} + \beta_{xyy} + \beta_{xzz}\right)^2 + \left(\beta_{yyy} + \beta_{xxy} + \beta_{yzz}\right)^2 + 6\alpha_{xz}^2 + 6\alpha_{xy}^2 + 6\alpha_{yz}^2\right] \quad (5)$$

Table 5 Dipole moment, mean, first and second hyperpolarizability of all compounds (computed by B3LYP and M06 functionals) and urea in the gas phase

	B3LYP in the gas phase					M06 in the gas phase				
	μ_0 in Debye	α_0 in 10^{-24}	$\Delta\alpha$ in 10^{-24}	β_o in 10^{-31}	$\overline{\gamma}$ in 10^{-37}	μ_0 in Debye	α_0 in 10^{-24}	$\Delta\alpha$ in 10^{-24}	β_o in 10^{-31}	$\overline{\gamma}$ in 10^{-37}
1a	3.55	13.227	18536	169.1	540.0	3.61	13.25	17965.33	151.18	504.48
1b	6.79	13.846	18869	203.3	598.9	6.97	13.81	18109.74	181.39	538.33
1c	2.70	27.691	22651	486.8	1443.5	2.85	26.85	22456.91	429.96	1351.14
1d	3.48	26.739	35398	361.4	1496.3	3.63	26.53	34027.52	313.20	1330.62
2a	1.93	9.1681	10621	131.2	336.5	2.03	9.16	10400.62	121.74	324.95
2b	5.09	10.055	11747	179.1	381.9	5.23	9.98	11233.44	161.83	352.07
2c	1.81	26.479	9865	297.5	613.6	1.88	26.10	9982.59	281.64	613.57
2d	1.84	24.442	23131	310.3	987.6	1.96	24.27	22476.14	279.45	918.77
3a	0.42	41.682	29308	161.0	4606.1	0.39	40.44	28204.63	135.52	4133.70
3b	0.05	41.682	30452	231.5	5505.5	0.11	40.91	28641.98	193.16	4647.77
3c	2.59	84.930	82347	2266.0	53791.7	2.07	60.84	45984.93	816.43	14183.87
Urea		3.830	2410	3.7	6.8		3.83	2409.95	3.71	6.76

$$\overline{\gamma} = (1/5)\left[\left(\gamma_{xxxx} + \gamma_{yyyy} + \gamma_{zzzz} + 2\gamma_{xxyy} + 2\gamma_{yyzz} + 2\gamma_{zzxx}\right)\right] \quad (6)$$

The values calculated for total static dipole moment (μ), the mean polarizability (α_0), the anisotropy of the polarizability (($\Delta\alpha$), the mean first hyperpolarizability (β), and static second hyperpolarizability (γ), of the eleven compounds using Eqs. 1, 2, 3, 4 and 5 are listed in Tables 5 and 6. More details are provided in the supporting information). The computed values for the first hyperpolarizability β_o for the compounds **1a-1d** were found to be greater than urea (3.71028×10^{-31}) by 45, 55, 131 and 97 times respectively using the B3LYP functional in the gas phase. The values obtained from the M06 functional are 40, 49, 115 and 84 times greater in the gas phase. In dichloromethane, the β_o values are found to be 73, 74, 284 and 141 times (B3LYP functional) and 64, 63, 237and 117 (M06 functional) times greater compared to the gas phase. As expected, these derivatives have shown a large hyperpolarizability values, suggesting considerable charge transfer characteristics of the first excited state which is also supported by the large difference in the dipole moments. The twisted structures of compounds **1c** (fused of naphthalene anhydride and naphthalene diamine) and **1d** (fused of naphthalene anhydride and phenantherene diamine) may account for this difference on comparing with compounds **1a** and **1b**. The

Table 6 Dipole moment, mean, first and second hyperpolarizability values of all compounds in dichloromethane computed by B3LYP and M06 functionals

	B3LYP/6-31G(d)					M06/6-31G(d)				
	μ_0 in Debye	α_0 in 10^{-24}	$\Delta\alpha$ in 10^{-24}	β_o in 10^{-31}	$\overline{\gamma}$ in 10^{-37}	μ_0 in Debye	α_0 in 10^{-24}	$\Delta\alpha$ in 10^{-24}	β_o in 10^{-31}	$\overline{\gamma}$ in 10^{-37}
1a	4.924	17.89	33580.78	273.03	1658.5	5.084	18.02	32605.4	240.81	1528.25
1b	8.801	18.30	33205.44	277.85	1638.0	9.004	18.32	31732.6	236.01	1449.85
1c	3.841	37.65	43029.66	1054.68	5165.0	4.035	36.49	42221.7	880.61	4529.13
1d	4.766	36.77	61965.26	526.16	4126.2	4.944	36.48	59409.0	435.07	3597.71
2a	2.580	11.96	18700.48	255.15	1036.4	2.711	11.98	18221.0	229.25	974.95
2b	6.349	12.94	19490.07	295.20	1066.4	6.500	12.84	18528.1	257.61	960.75
2c	2.309	36.63	18160.29	755.35	2298.5	2.403	36.05	18280.0	695.33	2220.10
2d	2.404	21.04	44613.77	545.50	2917.7	2.526	20.98	43145.6	471.10	2632.80
3a	0.269	55.16	56202.39	414.91	15991.0	0.199	52.97	53672.7	337.35	13479.60
3b	0.180	54.67	55323.79	503.66	16090.4	0.259	52.01	51686.6	405.34	12804.24
3c	2.701	86.74	102752.80	2747.15	67804.1	2.590	84.93	82347.8	2266.53	53791.71

planar structures of compounds **1a** and **1b** have electron density is delocalized over the molecule in the HOMO while in the LUMO, the electron density is localized on the anhydride moiety which is acting as an acceptor (supporting information). However, for the twisted structures of compounds **1c** and **1d**, the electron density of the HOMO is localized on the diamine moiety while in the LUMO, the electron density is localized on the anhydride moiety (supporting information), thus, restricting the conjugation path. Similar results are found in case of the compounds **2a**-**2d** and **3a**-**3c**. Despite that compounds **2a**-**2d** are planar, compound **2c** has highest hyperpolarizability. On considering compounds **3a**-**3c**, it is found that compound **3c** (twisted geometry) has the highest β_o value as computed by both the functionals in the gas phase and in dichloromethane. The overall reason for the large charge separation in the excited state may be due to the fused six membered amide ring (Fig. 1) of the compounds **1c**, **1d**, **2c** and **3c**. These compounds have a tetrahedral nitrogen atom acting as donor which is quite difficult situation in five membered fused ring derivatives as in the remaining compounds. The twisting in case of the compounds **1c**, **1d** and **3c** makes this effect more pronounced making HOMO localized and not spread all over the molecule. Another important observation is that in dichloromethane hyperpolarizability values are greater (by 2–3 folds) compared to gas phase suggesting better stabilization of charges in the excited state. These results suggest that the investigated compounds can be good candidates for organic NLO materials.

Conclusions

We studied the photophysical, electrochemical and NLO properties of eleven polycyclic benzimidazole dyes using two computational methods namely B3LYP/6-31G(d) and M06/6-31G(d). The ground and excited states geometries are well explained by both methods. The vertical excitations and emissions are computed and compared with the experimental values. These compounds have shown prominent absorption at the longer wavelength due to the HOMO→LUMO transition with higher oscillator strengths using the TD-M06/6-31G(d) method as compared to the TD-B3LYP/6-31G(d) method. The computed absorption and emission wavelengths are in fairly good agreement with the experimental values. The M06 functional performs better in the prediction of the electronic vertical excitation and emission properties compared to the popular B3LYP functional. This can be due to the fact that these compounds have large long range interactions arising from the dispersion of π electrons and the charge transfer. The electrochemical properties are also interpreted in terms of HOMO and LUMO energies using both methods. This theoretical data also indicates that the fluoro-derivatives have higher electron affinity which is necessary for better electronic transportation. The first hyperpolarizability was calculated using finite field approach and it was found that these compounds possess a large second-order nonlinear property which is attributed to the excited state intramolecular charge transfer. In summary, this paper describes the importance of the DFT method (B3LYP and M06 functionals) in understanding the photophysical and the electrochemical behavior at molecular level of polycyclic benzimidazole dyes for their applications in in organic electronics. The results shall prove to be significant in envisaging new structures consisting of these types of chromophoric systems.

Acknowledgments and Ethical Statement UW is thankful to UGC-SAP for financial support. LR and PR acknowledge the facilities from the University of Mauritius. The authors would like to thank the reviewers for their useful comments to improve the manuscript.

References

1. Herbst W, Hunger K, Wilker G, Heinfred Ohleier RW (2004) Industrial organic pigments: production, properties, applications, 3rd Edition. Ind Org Pigment. doi: 10.1002/3527602429
2. Mizuguchi J (2004) Crystal structure and electronic characterization of trans - and cis -perinone pigments. J Phys Chem 8926–8930
3. Li Y, Zhang G, Yang G et al (2013) Extended π-conjugated molecules derived from naphthalene diimides toward organic emissive and semiconducting materials. J Org Chem 78:2926–34. doi:10.1021/jo302677k
4. Mishra A, Fischer MKR, Bäuerle P (2009) Metal-free organic dyes for dye-sensitized solar cells: from structure: property relationships to design rules. Angew Chem Int Ed Engl 48:2474–99. doi:10.1002/anie.200804709
5. Zhan X, Facchetti A, Barlow S et al (2011) Rylene and related diimides for organic electronics. Adv Mater 23:268–84. doi:10.1002/adma.201001402
6. Zhao Y, Di C, Gao X et al (2011) All-solution-processed, high-performance n-channel organic transistors and circuits: toward low-cost ambient electronics. Adv Mater 23:2448–53. doi:10.1002/adma.201004588
7. Singh VP, Singh RS, Parthasarathy B et al (2005) Copper-phthalocyanine-based organic solar cells with high open-circuit voltage. Appl Phys Lett 86:82103–82106
8. Dhagat P, Haverinen HM, Kline RJ et al (2009) Influence of dielectric surface chemistry on the microstructure and carrier mobility of an n-type organic semiconductor. Adv Funct Mater 19:2365–2372. doi:10.1002/adfm.200900298
9. Hu Y, Gao X, Di C, et al (2011) Core-expanded naphthalene diimides fused with sulfur heterocycles and end-capped with electron-withdrawing groups for air-stable solution-processed n-channel organic thin film transistors. 1204–1215
10. Xue J, Uchida S, Rand BP, Forrest SR (2004) Asymmetric tandem organic photovoltaic cells with hybrid planar-mixed molecular heterojunctions. Appl Phys Lett 85:5757–5759
11. Ahmed E, Ren G, Kim FS, et al (2011) Design of new electron acceptor materials for organic photovoltaics: synthzesis, electron transport, photophysics, and photovoltaic properties of oligothiophene-functionalized naphthalene diimides. 4563–4577
12. Tang CW (1986) Two-layer organic photovoltaic cell. Appl Phys Lett 48:183–185

13. Babel A, Jenekhe SA (2003) High electron mobility in ladder polymer field-effect transistors. J Am Chem Soc 125:13656–7. doi:10.1021/ja0371810
14. Baeg K-J, Khim D, Jung S-W et al (2012) Remarkable enhancement of hole transport in top-gated N-type polymer field-effect transistors by a high-k dielectric for ambipolar electronic circuits. Adv Mater 24:5433–9. doi:10.1002/adma.201201464
15. Chang J, Ye Q, Huang K, et al (2012) Stepwise cyanation of naphthalene diimide for n-channel field-effect transistors. 2010–2013
16. Sophy KB, Calaminici P, Pal S (2007) Density functional static dipole polarizability and first-hyperpolarizability calculations of Nan (n = 2, 4, 6, 8) clusters using an approximate CPKS method and its comparison with MP2 calculations†. J Chem Theory Comput 3:716–727. doi:10.1021/ct6003627
17. Mamada M, Perez-Bolivar C, Anzenbacher P Jr (2011) Green synthesis of polycyclic benzimidazole derivatives and organic semiconductors. Org Lett 13:4882–4885
18. Frisch MJ, Trucks GW, Schlegel HB, Scuseria GE, Robb MA, Cheeseman JR, Scalmani G, Barone V, Mennucci B, Petersson GA, Nakatsuji H, Caricato M, Li X, Hratchian HP, Izmaylov AF, Bloino J, Zheng G, Sonnenberg JL, Hada M, Ehara M, Toyota K, Fukuda R, Hasegaw CJ, Fox DJ (2010) Gaussian 09 revision C01
19. Dooley R, Milfeld K, Guiang C et al (2006) From proposal to production: lessons learned developing the computational chemistry Grid cyberinfrastructure. J Grid Comput 4:195–208
20. Treutler O, Ahlrichs R (1995) Efficient molecular numerical integration schemes. J Chem Phys 102:346–354
21. Becke AD (1988) Density-functional exchange-energy approximation with correct asymptotic behavior. Phys Rev A 38:3098–3100
22. Becke AD (1993) Density-functional thermochemistry. III. The role of exact exchange. J Chem Phys 98:5648–5652
23. Lee C, Yang W, Parr RG (1988) Development of the Colle-Salvetti correlation-energy formula into a functional of the electron density. Phys Rev B 37:785–789
24. Stephens PJ, Devlin FJ, Chabalowski CF, Frisch MJ (1994) Ab initio calculation of vibrational absorption and circular dichroism spectra using density functional force fields. J Phys Chem 98:11623–11627. doi:10.1021/j100096a001
25. Becke AD (1993) A new mixing of Hartree–Fock and local density-functional theories. J Chem Phys 98:1372–1377
26. Xu X, Goddard WA (2004) The X3LYP extended density functional for accurate descriptions of nonbond interactions, spin states, and thermochemical properties. Proc Natl Acad Sci USA 101:2673–2677. doi:10.1073/pnas.0308730100
27. Perdew JP, Ziesche P, Eschig H (1991) In electronic structure of solids, 91st edn. Akademie Verlag, Berlin
28. Zhao Y, Truhlar DG (2007) The M06 suite of density functionals for main group thermochemistry, thermochemical kinetics, noncovalent interactions, excited states, and transition elements: two new functionals and systematic testing of four M06-class functionals and 12 other function. Theor Chem Accounts 120:215–241. doi:10.1007/s00214-007-0310-x
29. Zhao Y, Truhlar DG (2008) Computational characterization and modeling of buckyball tweezers: density functional study of concave-convex pi…pi interactions. Phys Chem Chem Phys 10:2813–8. doi:10.1039/b717744e
30. Tomasi J, Mennucci B, Cammi R (2005) Quantum mechanical continuum solvation models. Chem Rev 105:2999–3093. doi:10.1021/cr9904009
31. Cossi M, Barone V, Cammi R, Tomasi J (1996) Ab initio study of solvated molecules: a new implementation of the polarizable continuum model. Chem Phys Lett 255:327–335. doi:10.1016/0009-2614(96)00349-1
32. Hehre WJ, Radom L, von Schleyer R, Pople J (1986) Abinitio molecular orbital theory. Wiley, New York
33. Bauernschmitt R, Ahlrichs R (1996) Treatment of electronic excitations within the adiabatic approximation of time dependent density functional theory. Chem Phys Lett 256:454–464. doi:10.1016/0009-2614(96)00440-X
34. Furche F, Rappoport D (2005) Density functional methods for excited states: equilibrium structure and electronic spectra. Theor Comput Chem 16:93–128
35. Valeur B (2001) Molecular fluorescence: principles and applica-tions
36. Chibani S, Charaf-eddin A, Mennucci B, et al (2013) Optical signatures of OBO fluorophores: a theoretical analysis
37. Pohl R, Montes VA, Shinar J, Jr PA (2004) Red - green - blue emission from Tris (5-aryl-8-quinolinolate) Al (III) complexes stability and emission-color purity. The major obstacle in the fabrication of SMOLED-based full color displays is the so far limited availability of complexes that span. J Org Chem 1723–1725
38. Pohl R, Anzenbacher P (2003) Emission color tuning in AlQ 3 chromophores. Org Lett 213
39. Dennington R, Keith TMJ (2009) GaussView version 5
40. Castet F, Pic A, Champagne B (2014) Dyes and pigments linear and nonlinear optical properties of arylvinyldiazine dyes: a theoretical investigation. Dyes Pigments 110:256–260. doi:10.1016/j.dyepig.2014.03.021
41. Kaino BT, Tomaru S (1993) Organic materials for nonlinear optics **
42. Vidya S, Ravikumar C, Joe IH, et al (2011) Vibrational spectra and structural studies of nonlinear optical crystal ammonium D, L -tartrate: a density functional theoretical approach 2010:676–684. doi:10.1002/jrs.2743
43. Kleinman DA (1977) Nonlinear dielectric polarization in optical media. Phys Rev 1977–1979.
44. Franc J, Lacroix PG, Farfa N, et al. (2006) Synthesis, characterization and nonlinear optical (NLO) properties of a push – pull bisboronate chromophore with a potential electric field induced NLO. 2913–2920. doi: 10.1039/b606359d